Control of a fast NC axis with a crank mechanism

Ing. Štěpán Fiala

Supervisor: Ing. Jan Machyl, Ph.D

Abstract

Práce se zabývá zhodnocením běžně užívaných možností obrábění oválných profilů pístů, jakož i technologiemi, které se teprve v průmyslu objevují. Práce se dále věnuje matematickému modelování zvoleného klikového mechanismu, simulováním regulačního schématu celé NC osy a realizací zpětnovazebního zapojení na skutečném stroji. Následně byl matematický model na základě naměřených hodnot verifikován.

Keywords

Klikový mechanismus, řízení, regulace, ovalita pístu.

1. Introduction

This thesis aims to construct a mathematical model of a testing stand of a fast NC axis with a crank mechanism including a regulatory scheme and to compare a simulation model quality on a real machine using a measured transient response. It was necessary to assemble a regulatory scheme including a position loop, a speed loop and a current loop. The mathematical model of the crank mechanism has been processed in the Simulink graphical block diagramming tool and the model has been verified afterwards. A mathematical model assembled using a different method has been used in the verification process. The model has been assembled in the SimMechanics module based on the mechanism's topology and geometry. Because of the same input parameters, it was possible to verify modules assembled by this method. This implies that the axis has been produced and precisely adjusted earlier within the grant project. The production documentation was not available at that time, though, and because of the precise setting of the axis, it was impossible to disassemble the axis for the purpose of measuring physical parameters of the individual components. To estimate mass and moment of inertia, a 3D model of the components was used. Inclusion of the mathematical model into the regulatory scheme with a DC motor made it possible to proceed to a tuning of the regulators and to a measuring of the monitored variables. The characteristics created this way could be further verified by measuring on a real machine.

2. Machining oval profiles

2.1 Oval profiles of piston skirts

The reason why it is necessary to address the issue of machining oval profiles is apparent from a figure of a combustion engine piston of a Russian Dnepr motorcycle [4]. It is a revised drawing of a 60-year-old motorcycle piston, but the complexity of machining work should be apparent enough. The progress in the motorcycle industry is significant, motor piston profiles have gone through many changes. A drawing of a contemporary is impossible to obtain, though. This is mostly because the value of the companies engaged in designing pistons is saved right in the piston skirt profile. The process of piston construction includes, among other things, complex modelling of heat transfer in material and a calculation of its thermal expansion.

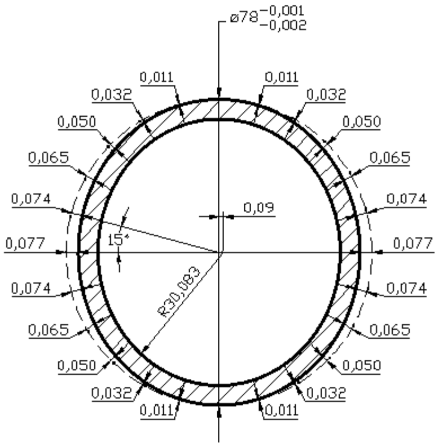

Fig. 1 *Oval piston profile [1]*

In the operating temperature of the engine, due to thermal expansion, a backlash of the oval piston and a cylinder occurs which causes a higher tightness of the workplace. A sample output of the measurement of the final product's shape is shown in *Fig. 2*. In the a) section, a change of the piston profile depending on the piston height is shown. For the sake of the diagram's clarity, the X and Y axes have been transposed. The dotted line shows the desired profile and the accurate piston ring groove in the height of approx. $36.6\ mm$. The two curves show a different piston profile for 0° and 180°. This difference is sufficiently evident from the top view of the piston showed in the b) section of the figure. The measurements have been taken within an evaluation of the project dealing with development of a highly dynamic machine for machining oval profiles of pistons. Bibliography [2] deals with a development of a machine with piezoelectric actuation of high momentum, long stroke, high rigidity and repeatable positioning accuracy. The actuation should also meet requirements for a transfer of high cutting forces in machining and a fast response to control signals. The entire unit was designed with regard to a compact size and a modularity of the system. It is therefore possible to equip an ordinary CNC lathe with such module.

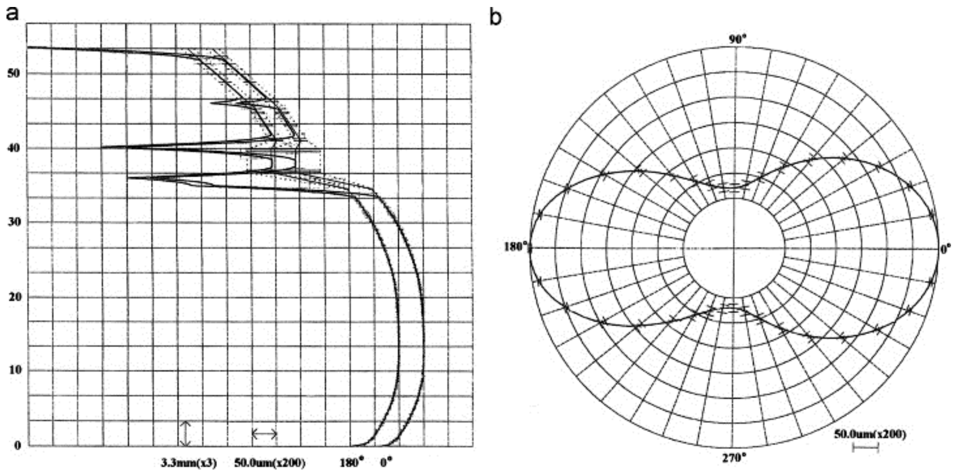

Fig. 2 *Measurement result of piston ovality[2]*

2.2 Machine manufacturers mechanisms

The manufacturer of the machine tools equipped with the piezoelectric actuator for machining non-cylindrical profiles is the Takisawa company [5]. The patent's abstract related to these machines shows a kinematic diagram of the actuator (*Fig. 3*).

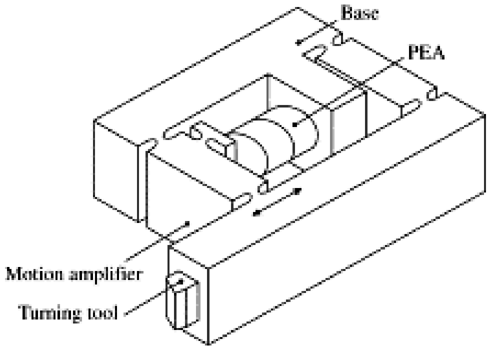

Fig. 3 *Diagram of piezoelectric actuator[5]*

The picture shows both important mechanism parts and functions. The piezoelectric actuator attached to the base transmits power to the tool holder by parallel elastic elements. A lever in the first element of a parallelogram provides some transfer. The unit construction made of a single piece of material eliminates possible looseness in the mechanism, but it is highly demanding on the material and design of rotating flexible links. These throttlings are very important in the analysis of a cyclically stressed material fatigue.

Another concept of the piezoelectric actuator is a machine of the Cedrat Technologies company [6]. Again, the piezoelectric crystal is fixed between flexibly deformed arms multiplying the crystal's lift, which is, in this case, accomplished by a flexibly deformed scissor mechanism.

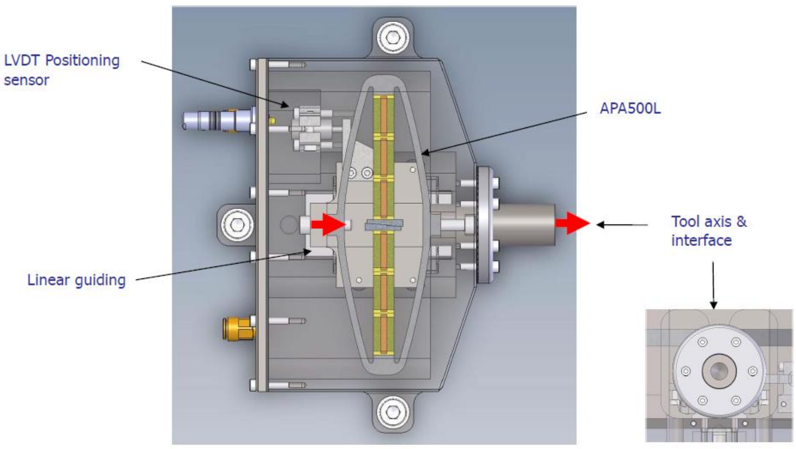

Fig. 4 *SPT500L with piezoelectric actuator APA 500L APA 500L [6]*

Maximum achieved force is 500N, stroke is 570 µm and accuracy is below 1 µm. Development of this module, which can be mounted directly on the turret of turning center, lasted six months. In result, in combination of Z and X axes, turning center can machine both the conical piston in a standard way and its oval shape with help of additional high-frequency axis SPT. The stripped structure of the additional module is shown in *Fig. 4*.

3. Solution of axis with crank mechanism

Based on an assessment of possible realizations of rotary motion transmitted in translational motion, the crank mechanism was chosen in the grant project [3]. In the grant project, using the same motor, a draft calculation of a mechanism with a ball-screw has been processed. However, NC axis with the crank mechanism reached a theoretical acceleration of $a=72.38ms^{-2}$, which was approximately *3.5* times greater.

3.1 Assembling a motion equation of crank mechanism

To create a regulatory scheme of the entire axis, it is primarily necessary to mathematically describe the crank mechanism. There are several methods to assemble motion equations of a centric crank mechanism which is shown on *Fig. 5*. These are eg. the d'Alembert method of extraction, the virtual work principle, the Lagrange method of equations of the second kind, and the method of reduction of mass and force quantities [1].

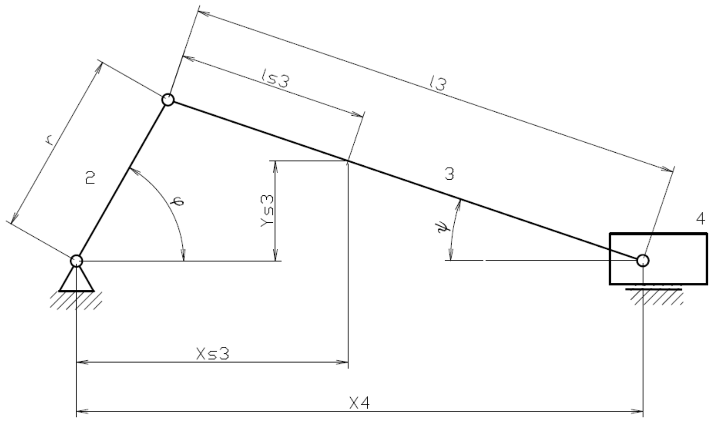

***Fig. 5** Centric crank mechanism*

To assemble the motion equation of the given crank mechanism, the method of reduction of mass and force quantities is used.

$$M^*_{(q)}\ddot{q} + \frac{\dot{q}^2}{2}\frac{dM^*_{(q)}}{dq} = Q \tag{1}$$

Considering the crank mechanism actuation (*Fig. 5*), the φ rotation of the crankshaft was chosen as the generalized q coordinate. Reducing the system to a rotary element thus implies the following shape of the motion equation:

$$I_{RED}\ddot{\varphi} + \frac{\dot{\varphi}^2}{2}\frac{dI_{RED}}{d\varphi} = M_{RED} \tag{2}$$

I_{RED} is a reduced moment of motor rotor inertia, M_{RED} is a reduced torque. To assemble a simulation model, it is preferable to convert the equation (2) to this form:

$$\ddot{\varphi} = (M_{RED} - \frac{\dot{\varphi}^2}{2}\frac{dI_{RED}}{d\varphi})/I_{RED} \tag{3}$$

The calculation of a reduced inertia moment is based on the König's theorem as follows:

$$I_{RED} = I_K + I_E + I_3\frac{\dot{\psi}^2}{\dot{\varphi}^2} + m_3(\frac{\dot{x}_{s3}^2}{\dot{\varphi}^2} + \frac{\dot{y}_{s3}^2}{\dot{\varphi}^2}) + m_4\frac{\dot{x}_4^2}{\dot{\varphi}^2} \tag{4}$$

The following conversions are introduced to simplify the coefficient calculations:

$$\frac{\dot{\psi}^2}{\dot{\varphi}^2} = p_3^2 \qquad\qquad \frac{\dot{x}_{s3}^2}{\dot{\varphi}^2} = p_{sx}^2 \tag{5}$$

$$\frac{\dot{y}_{s3}^2}{\dot{\varphi}^2} = p_{sy}^2 \qquad\qquad \frac{\dot{x}_4^2}{\dot{\varphi}^2} = p_4^2$$

Excluding the parameter of φ rotation of the crankshaft using kinematic conditions of the crank mechanism enabled acquiring the complete motion equation of the crank mechanism. This equation can be further interpreted in the Simulink environment (*Fig. 6*).

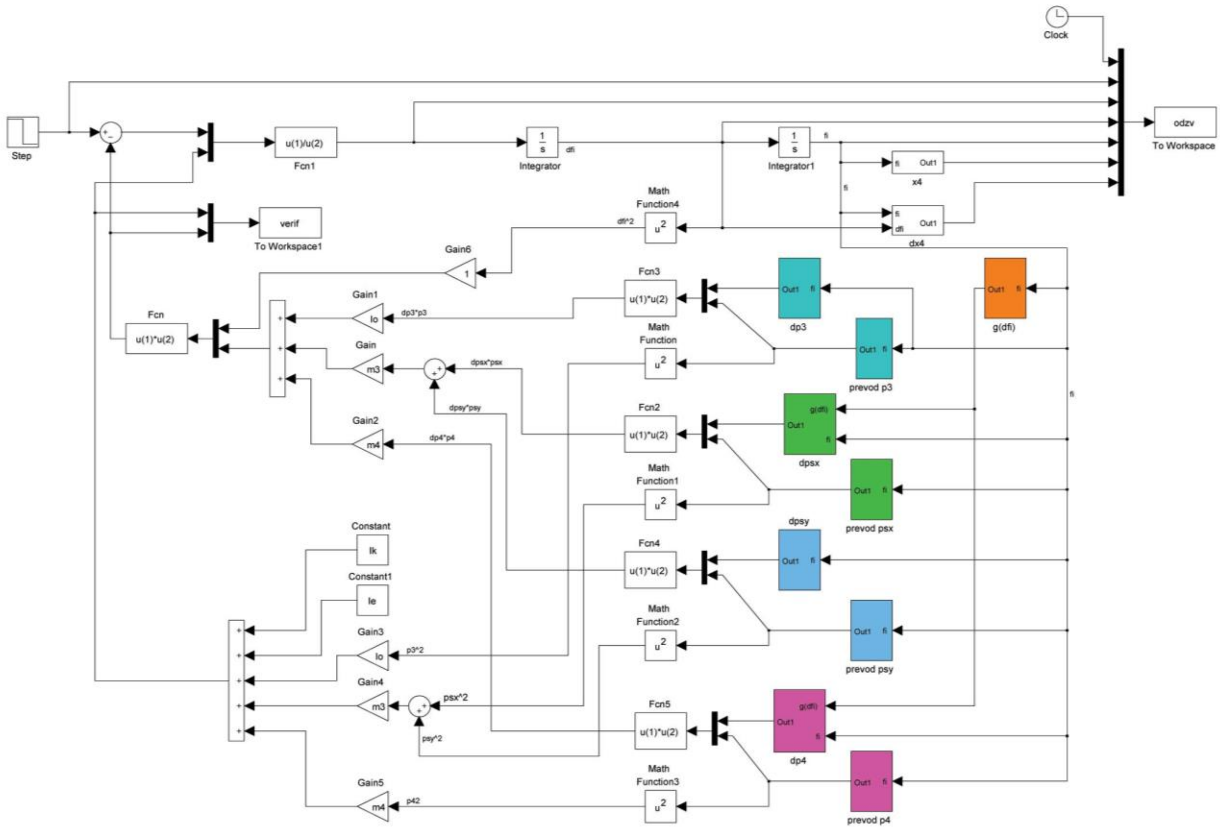

Fig. 6 *Motion equation of crank mechanism [1]*

The colored subsystems represent conversions defined in the equations (5) and their time derivations. This mathematical model needs verification. It was accomplished by a SimMechanics toolbox. Topology and the MBS (Multi Body System) parameters enable a quick assembly of mathematical models even in complex tasks.

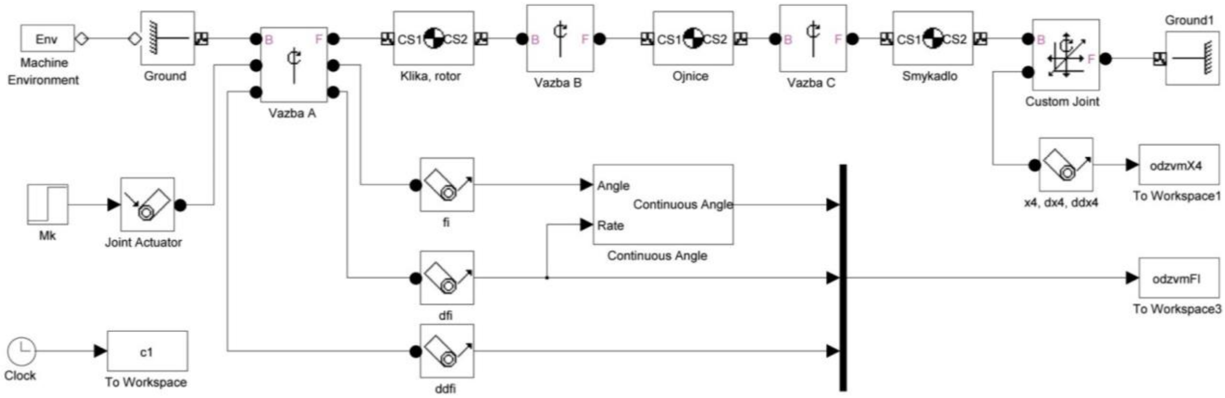

Fig. 7 *The crank mechanism model in SimMechanics [1]*

To reach the same mechanism parameters, a simulation was executed and the results compared. The mathematical models are the same with almost no deviations, so the model assembled using the reduction method can be assumed correct.

3.2 Assembling the regulatory scheme of the NC axis

After assembling the mathematical model of the crank mechanism, it is possible to implement it in a regulatory scheme. *Fig. 8* shows this block as an„$M - model$“. The block represents a single-mass system connected to a regulatory scheme of a brush DC motor with a control loop of position, velocity and current and with a feedforward velocity loop. The „$M - model$“ subsystem features fi and dfi pins, used in a feedback connection of a proportional position controller and a proportional integral velocity controller. Feedback current of the PI current controller is collected next to the motor model after a transfer function„$Fcn1$“.

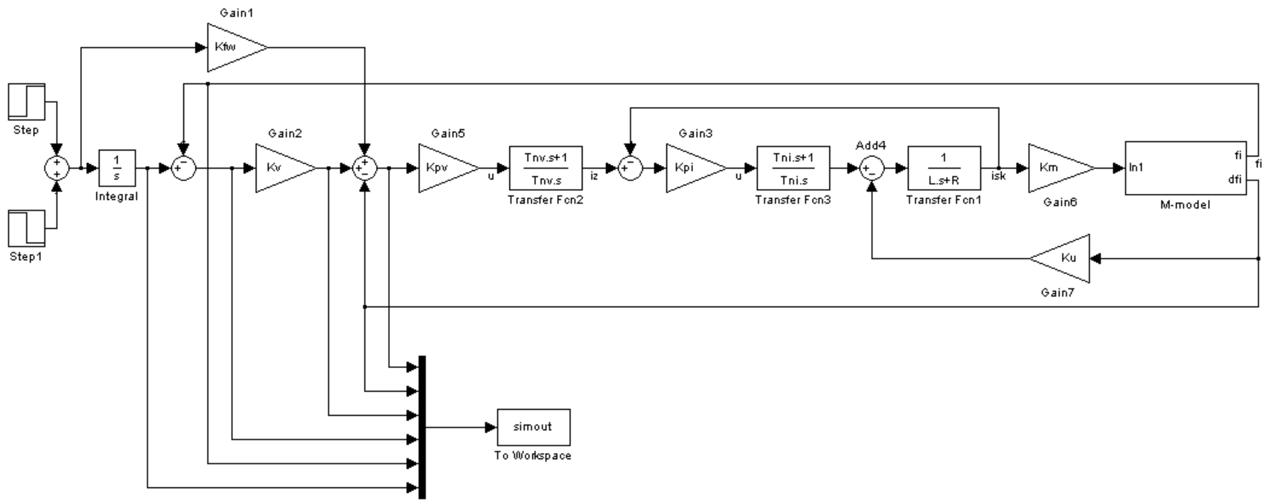

Fig. 8 *Simulation model of NC axis with a crank mechanism [1]*

A Mathlab/Simulink module – Real Time Toolbox – provides a real-time control of the NC axis with crank mechanism. The biggest advantage of the toolbox the fact it treats signal and data in the same manner as Simulink. The only difference is the mandatory adapter analog I/O definition. The scheme is apparent from *Fig. 9*, where „$RT\ Buf\ In$“ represents an input of Stegmann incremental sensor pulses in a resolution of $2500\ pulses/rev$. The positive direction of motor rotor is opposite to the positive direction of the incremental sensor. Therefore, the gain block after the pulse resolution block features a negative sign. The crankshaft rotation calculated by this method is connected to a position controller feedback. Next to it, there is a derivation to rotation velocity, which is connected to the velocity control feedback. The sum block also features a port for a velocity feedforward. After the PI velocity controller, there are blocks of voltage offset and voltage saturation as a security element. „$RT\ Out$“ represents the channel 1 of the analog adapter output.

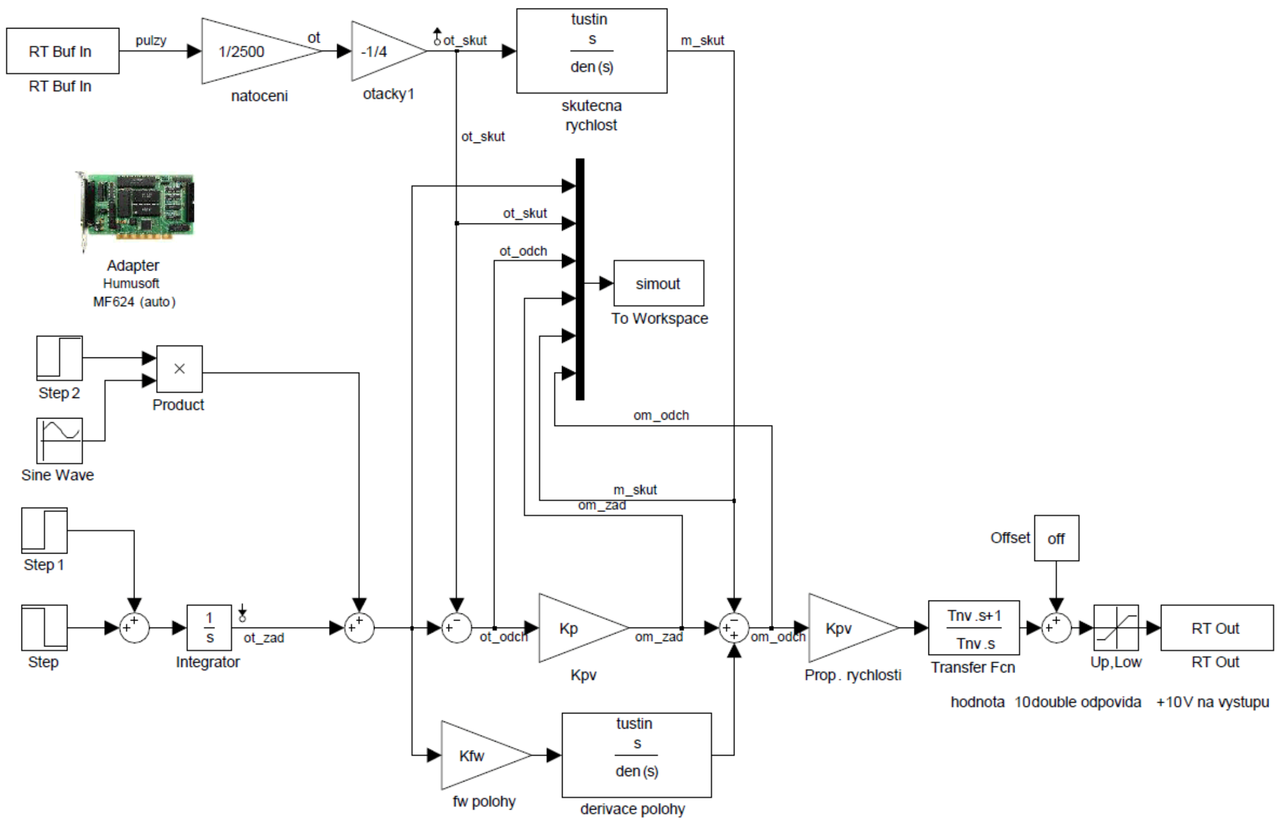

Fig. 10 Regulatory scheme of position controller and velocity controller of NC axis [1]

4. Comparison of measured and simulated data

Tuning the regulators of the lowest loop (current loop), the velocity loop and the position loop and putting the regulator parameters into the regulatory simulation scheme enables comparing transient response of a real control and a model. Two voltage amplifiers have been used while putting the NC axis into operation.

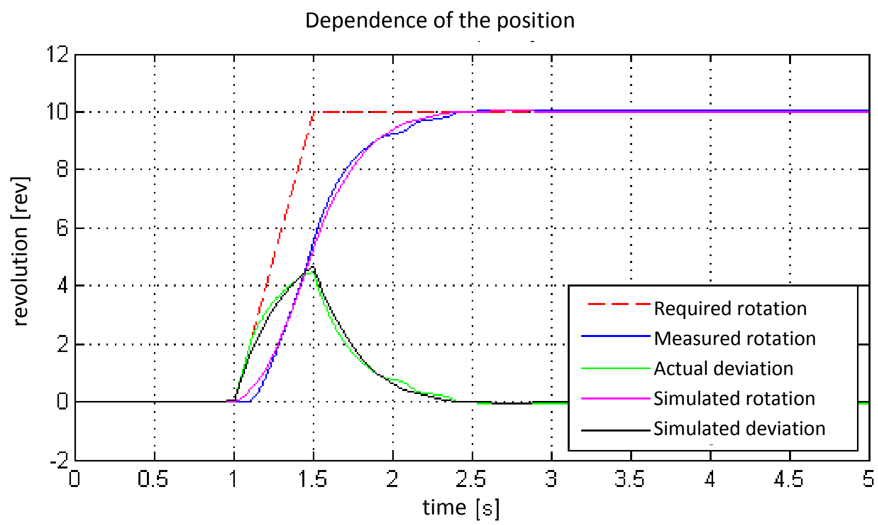

Fig. 11 Transient response and measuring (the Pololu amplifier [7]) [1]

There are two transient response of position combined in one chart on *Fig. 12*. It is possible to see a quite good quality of simulation model and nonlinear effects which are not included in the model. On actual position represented by blue line is shown start delay caused by coulomb friction and voltage dead zone ± *5.5 V* of amplifier even if the initial condition of position is given by $\varphi = 0$ („straight" mechanism, the minimum reduced moment of inertia). For this reason it was not possible to use the Pololu amplifier in position controlling.

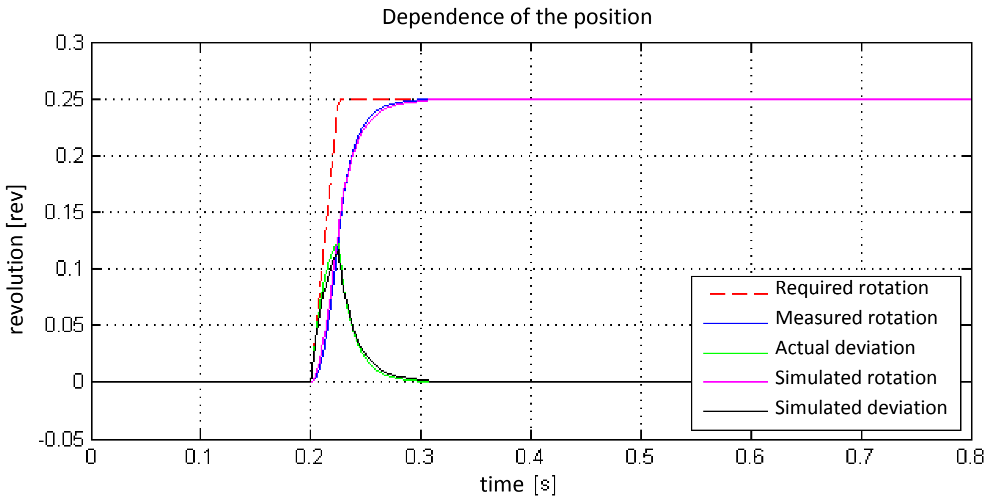

***Fig. 13** Transient response and measuring (The Junus amplifier [8]) [1]*

The Junus amplifier has no voltage dead zone near 0V and current control loop is included directly in the amplifier. Much better results were achieved for the same configuration of controllers.

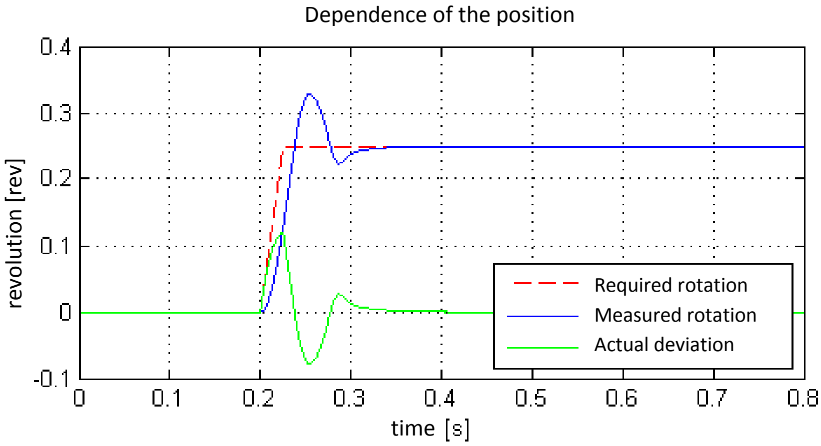

***Fig. 14** Transient response and measuring (The Junus amplifier [8]) [1]*

Maximum position deviation of simulation model and the real measurement is possible to read on *Fig. 15*. Deviation of the simulation model from the real measurement in percentage does not exceed 2%.
We get undesirable position overshoot of transient response when considerably higher K_v (position controller gain) is chosen. This overshoot is for $K_v = 150\ s^{-1}$ shown on *Fig. 16*. Initial conditions were considered as in all previous cases.

5. Conclusion

The thesis evaluates commonly used capabilities of machining oval pistons profiles and describes technologies emerging in the industry. The thesis also deals with mathematical modeling of a selected crank mechanism. The method of assembling the motion equations of crank mechanism was the method of reduction of mass and force quantities. Thus was constructed a mathematical description of the crank mechanism.

In the next step, a simulation of a regulatory scheme of the entire NC axis was performed and a feedback circuit in a real machine was implemented. The mathematical model has been subsequently verified upon the measured values.

The NC axis should only be operated in the area of crankshaft rotation, when the transfer mechanism is approximately constant. In such case, it would be possible to ignore the term representing the variable ratio of transfer function. Nevertheless, the machine should be equipped with an incremental sensor of the position of motor rotor, i.e. a sensor working in the whole revolution of the rotor. There was no reason to simplify the equation of motion mechanism. Parametrical mathematical model was assembled in environment of Simulink block diagrams editor. It was possible to make a partial verification of this model by comparing it with another model, which was assembled in SimMechanics. For relevant verification of mathematical model was necessary to make comparison between simulated results and measured result.

Symbol list

E_k	-	Kinetic energy	[J]
I_E	`Ie`	Moment of inertia of eccentric shaft	[kgm^2]
I_K	`Ik`	Moment of inertia of motor rotor	[kgm^2]
I_o	`Io`	Moment of inertia of connection rod	[kgm^2]
K_{fw}	`Kfw`	Velocity feedforward gain	[s^{-1}]
K_{pv}	`Kpv`	Velocity controller proportional gain	[s^{-1}]
K_v	`Kv`	Position controller proportional gain	[s^{-1}]
l_3	`l3`	Connection rod length	[m]
l_{s3}	`ls3`	Local distance of mass center of connection rod	[m]
m_i	-	Element weight	[kg]
M_k	`Mk`	Motor rotor torque	[Nm]
m_l	`ml`	Bearing weight	[kg]
$M^*_{(q)}$	-	Generalized mass	[kg]
M_{RED}	-	Reduced torque	[Nm]
m_3	`m3`	Connection rod weight	[kg]
m_4	`m4`	Slider weight	[kg]
p_{sx}	`psx`	Conversion function of connection rod mass center in x direction	[-]

p'_{sx}	dpsx	Derivative conversion function of connection rod mass center in x direction	[-]
p_{sy}	psy	Conversion function of connection rod mass center in y direction	[-]
p'_{sy}	dpsy	Derivative conversion function of connection rod mass center in y direction	[-]
p_3	p3	Conversion function of connection rod	[-]
p'_3	dp3	Derivative conversion function of connection rod	[-]
p_4	p4	Conversion function of slider	[-]
p'_4	dp4	Derivative conversion function of slider	[-]
q	–	Generalized coordinate	[rad,m]
$\dot{q}$	–	Generalized velocity	[rads^{-1}, ms^{-1}]
Q	–	Generalized forces	[N]
r	r	Radius of crank shaft	[m]
T_{ni}	Tni	Time constant of current controller	[s]
T_{nv}	Tnv	Time constant of velocity controller	[s]
v_i	–	Element velocity	[ms^{-1}]
x_{s3}	–	Global *x* coordinate of connection rod mass center	[m]
$\dot{x}_{s3}$	–	Global velocity of connection rod mass center in *x* direction	[m]
x_4	x4	*x* coordinate of slider stroke	[m]
$\dot{x}_4$	dx4	Linear slider velocity	[ms^{-1}]
y_{s3}	–	Global *y* coordinate of connection rod mass center	[m]
$\dot{y}_{s3}$	–	Global velocity of connection rod mass center in *y* direction	[ms^{-1}]
φ	fi	Revolution of crank shaft	[rad]
$\dot{\varphi}$	dfi	Rotation speed of crank shaft	[rads^{-1}]
$\ddot{\varphi}$	ddfi	Rotation acceleration of crank shaft	[rads^{-2}]
ψ	–	Connection rod revolution to mechanism axis	[rad]
$\dot{\psi}$	–	Velocity of connection rod revolution	[rads^{-1}]

List of used literature

[1] FIALA Š. *Control of a fast NC axis with a crank mechanism.* Prague : ČVUT in Prague, 2012.

[2] HAIFENG WANG, SHUYAN YANG. ScienceDirect.com - *Mechanical Systems and Signal Processing - Design and control of a fast tool servo used in noncircular piston turning process.* ScienceDirect.com. [Online] Elsevier, 3. 8. 2011. [Citace:4.5.2012.]

[3] SOUČEK P., CHMELA F. *Optimalizace a zvyšování dynamických vlastností pohonů posuvů.* Prague : ČVUT in Prague, 1997.

[4] HARVIN, CHARLIE. *Ural and Dnepr technical resources and links.* [Online] Good Karma Productions, 2008. [Citace: 4. 5. 2012.] http://www.goodkarmaproductions.com/html/tech.html.

[5] TAKISAWA MACHINE TOOL CO.,LTD. [Online] TAKISAWA MACHINE TOOL CO.,LTD., 2012. [Citace: 4. 5. 2012.] http://www.takisawa.co.jp.

[6] CEDRAT TECHNOLOGIES. *Mechatronic products.* [Online] CEDRAT TECHNOLOGIES, 16. 4. 2012. [Citace: 5. 5. 2012.] http://www.cedrat-technologies.com/en/about-us/contacts.html.

[7] POLOLU CORPORTION. *Pololu High-Power Motor Driver 24v23 CS.* [Online] Pololu Corporation, 2012. [Citace: 2. 6. 2012.] http://www.pololu.com/catalog/product/1456.

[8] COPLAY CONTROLS. *Junus* [Online] Coplay Controls, 2012. [Citace: 2. 6. 2012.] http://www.copleycontrols.com/motion/pdf/Junus.pdf.